The Astrophysical Journal, 686: L5–L8, 2008 October 10

A NOVEL METHOD FOR MEASURING THE EXTRAGALACTIC BACKGROUND LIGHT: *FERMI* APPLICATION TO THE LOBES OF FORNAX A

Markos Georganopoulos,[1,2] Rita M. Sambruna,[2] Demosthenes Kazanas,[2] Analia N. Cillis,[2] Chi C. Cheung,[2] Eric S. Perlman,[3] Katherine M. Blundell,[4] and David S. Davis[1,2]

Received 2008 May 30; accepted 2008 August 27; published 2008 September 16

ABSTRACT

We describe a new method for measuring the extragalactic background light (EBL) through the detection of γ-ray inverse Compton (IC) emission due to scattering of the EBL photons off relativistic electrons in the lobes of radio galaxies. Our method has no free physical parameters and is a powerful tool when the lobes are characterized by a high-energy sharp break or cutoff in their electron energy distribution (EED). We show that such a feature will produce a high-energy IC "imprint" of the EBL spectrum in which the radio lobes are embedded and show how this imprint can be used to derive the EBL. We apply our method to the bright nearby radio galaxy Fornax A, for which we demonstrate, using *Wilkinson Microwave Anisotropy Probe* (*WMAP*) and EGRET observations, that the EED of its lobes is characterized by a conveniently located cutoff, bringing the IC EBL emission into the *Fermi Gamma-Ray Space Telescope* energy range. We show that *Fermi* will set upper limits to the optical EBL and measure the more elusive infrared EBL.

Subject headings: diffuse radiation — galaxies: active — quasars: general — radiation mechanisms: nonthermal — X-rays: galaxies

1. INTRODUCTION

The EBL that permeates the universe in the optical-IR is closely connected to the history of structure formation. It is composed of the cosmic infrared background (CIB) peaking at $\lambda \sim 100$ μm (dust-reprocessed starlight) and the cosmic optical background (COB) peaking at $\sim$1 μm (starlight), and its level is still unknown to a factor of a few, due to the dominance of foregrounds such as the interplanetary dust emission and Galactic emission (Hauser & Dwek 2001; Kashlinsky 2005). Robust lower limits to the EBL level have been set by galaxy counts (e.g., Dole et al. 2006). Useful upper limits in the 1–10 μm range can be obtained by using the TeV blazar emission to set limits on the EBL by modeling its attenuation due to pair production with EBL photons (e.g., Stecker et al. 1992). This method assumes that the intrinsic blazar TeV spectrum cannot be arbitrarily hard (e.g., Aharonian et al. 2006). However, this can be circumvented (Katarzyński et al. 2006; Stecker et al. 2007; Aharonian et al. 2008), significantly relaxing the EBL limits derived (Mazin & Raue 2007).

We propose to measure the EBL by detecting the high-energy emission produced when EBL photons IC-scatter off the relativistic electrons of extragalactic sources. IC scattering of the cosmic microwave background (CMB) has already been detected in the X-rays from the lobes of a handful of radio galaxies (e.g., Erlund et al. 2008). In fact, the first confirmation for the presence of the CMB in an extragalactic location came from the *ROSAT* X-ray detection of the lobes of Fornax A by Feigelson et al. (1995). The idea we propose is based on the fact that, although the EBL energy density is only around a few percent that of the CMB, the CIB and COB photons have energies correspondingly $\sim$10 and 1000 times higher than those of the CMB. For a source with a given EED, its electrons will IC-scatter the CMB and EBL photons, and the IC emission will have a spectral shape related to that of the CMB and EBL, shifted in frequency by $\gamma_{\rm max}^2$, where $\gamma_{\rm max}$ is the maximum Lorentz factor of the EED. Therefore, the IC emission from such a source will consist of a powerful component due to CMB seed photons and two weaker components with a power of a few percent that of the CMB one but shifted in energy by a factor of $\sim$10 and 1000. The cleanest spectral separation of these IC components results from a power-law EED characterized by a high-energy cutoff.

If this IC emission can be detected, we will observe the high-energy imprint of the CMB+EBL at the location of our source. This imprint will provide us with the level and spectral shape of the CIB+COB at the source. Here we show that the lobes of radio galaxies, if characterized by an EED with a suitably located high-energy cutoff, can be used to measure the EBL at their location through *Fermi* observations, and we demonstrate our method on the radio lobes of the nearby bright radio galaxy Fornax A.

2. EBL γ-RAY IMPRINTS: THE CASE OF FORNAX A

We exclude blazars and radio quasars, whose GeV emission is dominated by their parsec-scale jet IC emission. The favored sources are the extended lobes of radio galaxies with weak active galactic nuclei (AGNs) that are not expected to be significant GeV emitters. Moreover, weak AGNs will not contribute optical-IR seed photons to the radio lobes, beyond those contributed by the host galaxy. In addition to the lobe synchrotron radio emission, the lobe IC emission off the CMB must also be detected, to determine the lobe magnetic field and the EED normalization, *without resorting to the equipartition assumption. This parameter-free determination of the EED is necessary for a one-to-one mapping of the EBL to its IC emission.* The only cases for which IC off the CMB has been unambiguously identified is the X-ray emission of the lobes of a handful of radio galaxies. Given that in these sources the X-ray spectral index $\alpha_{\rm X} < 1$, the peak of the IC emission off the CMB is at higher energies, and the peak of the IC emission of the CIB and COB is at energies $\sim$10 and 1000 times higher correspondingly. The peak energy of the three IC components $\propto \gamma_{\rm max}^2$. This means that the only energy range at which we could expect to detect the IC emission off the CIB and COB is the GeV energy range covered by *Fermi*, and this for a relatively narrow range of $\gamma_{\rm max} \sim 10^5$ that keeps the IC off the CMB below the 100 MeV lower energy threshold of

[1] Department of Physics, Joint Center for Astrophysics, University of Maryland, Baltimore County, Baltimore, MD.
[2] Astrophysics Science Division, NASA Goddard Space Flight Center, Greenbelt, MD.
[3] Department of Physics and Space Sciences, Florida Institute of Technology, Melbourne, FL.
[4] Department of Physics, University of Oxford, Oxford, UK.

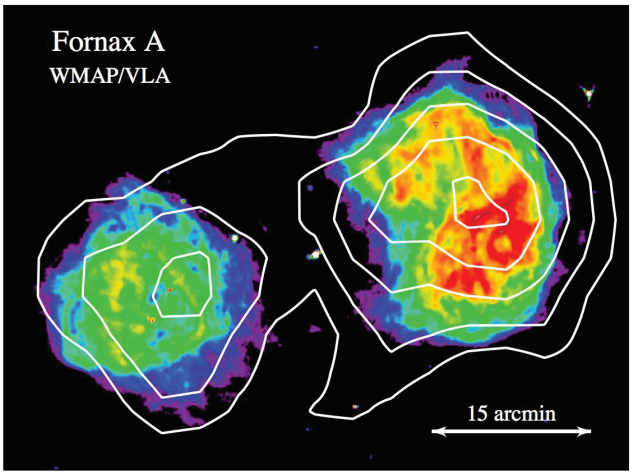

FIG. 1.—The 1.5 GHz VLA (*color*; Fomalont et al. 1989) and 61 GHz *WMAP* (*contours*; Hinshaw et al. 2007) images of Fornax A.

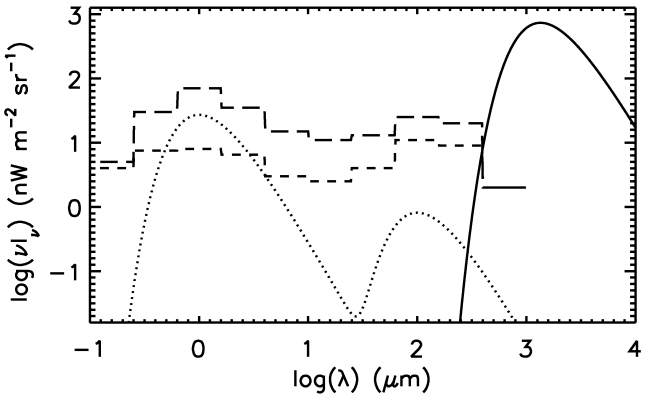

FIG. 2.—Seed photons at the lobes of Fornax A. *Solid line*: CMB. *Dotted line*: Host Galaxy. *Short-dashed line*: Low estimate of the EBL. *Long-dashed line*: High estimate of the EBL. The 1 and 100 μm peaking components due to the host galaxy have a total intensity of 36.7 and 1.1 nW m^{-2} sr^{-1}, respectively. In the low EBL case, the COB (liberally extending to $\lambda = 10$ μm) has an integrated intensity of 26.7 nW m^{-2} sr^{-1} and the CIB (10 μm $< \lambda <$ 10^3 μm) an integrated intensity of 26.2 nW m^{-2} sr^{-1}. In the high EBL case, the COB has an integrated intensity of 142.7 nW m^{-2} sr^{-1} and the CIB an integrated intensity of 72.8 nW m^{-2} sr^{-1}.

Fermi. Larger values would dominate the *Fermi* band by IC off the CMB, and smaller values would shift part or all of the IC off the EBL below the 100 MeV threshold. Sources that satisfy the $\gamma_{\rm max}$ constraint are required to have no other γ-ray source within *Fermi*'s angular resolution (~30′ at 1 GeV). A high Galactic latitude is desirable, because it reduces contamination from Galactic sources. Finally, high-frequency radio observations and existing EGRET limits of the γ-ray flux are needed to constraint the critical quantity $\gamma_{\rm max}$.

Fornax A is a high Galactic latitude (−57°) bright radio galaxy at a distance of 18.6 Mpc (5.41 kpc arcmin^{-1}), hosted by the massive elliptical NGC 1316 that shows a LINER core (Isobe et al. 2006). In the radio, it shows two relaxed lobes of ~20′ diameter separated by ≳30′ (Fig. 1). We use radio data collected by Isobe et al. (2006), replacing the extrapolated 100 MHz data point from Finlay & Jones (1973) with an 86 MHz measurement (Mills et al. 1960). We also use the integrated 3 yr *WMAP* fluxes (Hinshaw et al. 2007) from 23 to 61 GHz, which are larger than the 1 yr *WMAP* fluxes quoted by Cheung (2007). The total radio spectrum has a spectral index of $\alpha_r = 0.68 \pm 0.1$ (Isobe et al. 2006), increasing to ~0.8 in the *WMAP* band (Hinshaw et al. 2007). The western lobe is ~1.9 times brighter than the eastern in the Very Large Array (VLA) 1.5 GHz map, but this ratio is only ~1.3 in the *WMAP* 41 and 61 GHz maps. The lobes have been detected in X-rays by *ROSAT* (Feigelson et al. 1995) and *XMM* (only the eastern lobe was observed) with $\alpha_{\rm X} = 0.62^{+0.24}_{-0.15}$ (Isobe et al. 2006), consistent with the radio index α_r (here we assume $\alpha_r = \alpha_{\rm X} = \alpha = 0.65$). The lobe X-ray emission is due to IC-scattered CMB photons (the synchrotron self-Compton level is much below the observed flux). Because the CMB energy density is given, the X-ray flux and spectral index uniquely define the EED slope and normalization. With this at hand, the magnetic field required to produce the radio emission is uniquely determined to $B = 1.7$ μG, close to the equipartition field of $B = 1.55$ μG (Isobe et al. 2006).

EGRET provides a 2.2 σ detection at the 10^{-8} photons cm^{-2} s^{-1} level, for photons with energy $E > 100$ MeV (Cillis et al. 2004), which we treat as an upper limit for the total lobe flux. A cutoff is required in the lobe EED, otherwise the IC of the CMB emission would violate the EGRET upper limit. This constrains $\gamma_{\rm max} \lesssim (3\nu_{\rm EGRET}/4\nu_{\rm CMB})^{1/2} \sim 3 \times 10^5$, with the additional constraint that $\gamma_{\rm max}$ must be sufficiently high to extend the synchrotron emission to the *WMAP* energies, $\gamma_{\rm max} \gtrsim (\nu_{WMAP}/2 \times 10^6 B)^{1/2} \sim 10^5$. A fit of the combined constraints requires $\gamma_{\rm max} = 1.6 \times 10^5$, close to the optimal $\gamma_{\rm max} \sim 10^5$. The total lobe spectral energy distribution (SED) and the model SED is shown in Figure 3, where the dot-dashed line is IC emission off the CMB. Note that while none of the synchrotron and IC peaks are detected, their location is well constrained from the *WMAP* and EGRET data.

The electrons in the lobes will also experience the directional photon field of the host galaxy. The unknown source orientation affects the IC level through the angle of IC scattering (e.g., Brunetti et al. 1997; Dermer et al. 1992) and by determining the distance of the lobes from the host galaxy. The combined effect results in a θ-dependence of the total IC flux from both lobes due to galactic seed photons $f_{\rm IC,\,gal} \propto [(1 + \cos\theta)^2 + (1 - \cos\theta)^2] \sin\theta^2$, which has a flat maximum at $\theta = \pi/2$, remaining within 10% of the maximum for $\theta \gtrsim 60°$. We assume that the source axis forms an angle of $\theta = 60°$ to the line of sight, using an average lobe projected distance of 15′ from the galaxy. Given the flat θ-dependence of $f_{\rm IC,\,gal}$ for $\theta \gtrsim 60°$, our choice represents the maximum IC emission of the lobes due to host galaxy seed photons. The SED of the host galaxy (Dale et al. 2007) is comprised of two components, the first one peaking at ~1 μm, and the second one, ~30 times weaker, peaking at ~100 μm. We approximate its SED as the sum of two black bodies, and we plot in Figure 2 with a dotted line the resulting isotropic equivalent photon field intensity at the lobes.

For the EBL, we adopt a lower and an upper level (short- and long-dashed lines, respectively, in Fig. 2) of the expected background, by roughly following the range considered by Mazin & Raue (2007). This is meant to represent a plausible range of the yet unknown EBL. Without loss of generality, we choose to represent the EBL as a histogram for reasons that will become apparent in § 3. We note here that the lower limit is rather well established, because it relies on galaxy counts (e.g., Dole et al. 2006). As can be seen from Figure 2, the lobe photon field at $\lambda \lesssim 10$ μm has comparable contributions from the galaxy and the COB for all plausible COB levels, while at $\lambda \gtrsim 10$ μm and up to ~300 μm, the photon field is dominated by the CIB by more than a factor of 10, even for the lower EBL limit.

3. THE γ-RAY IMPRINT OF THE EBL

We present now the SED of the IC emission for the lower and higher EBL cases (lower and upper panels of Fig. 3). The

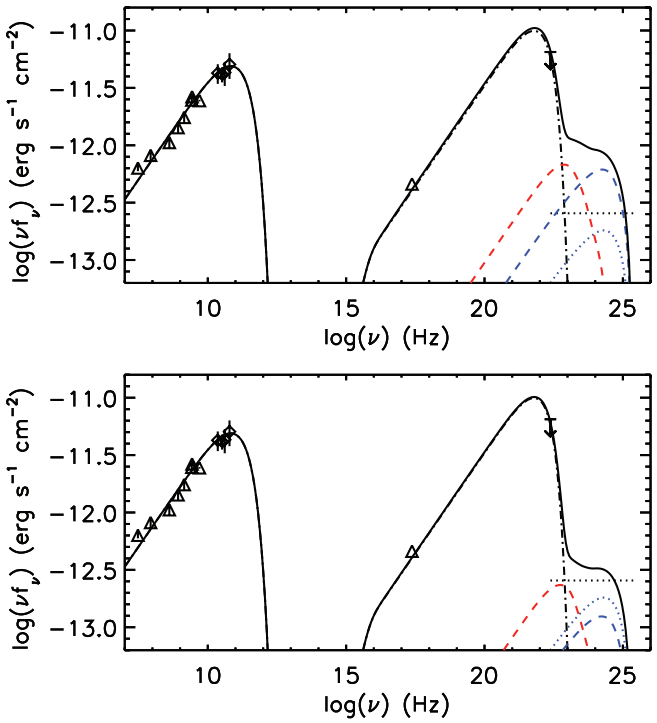

FIG. 3.—Radio, *WMAP*, and X-ray flux from both radio lobes, as well as the EGRET upper limit. The solid line is the model SED, resulting from a magnetic field of $B = 1.7$ μG, and a power-law EED with slope $p = 2.3$ and maximum Lorentz factor $\gamma_{max} = 1.6 \times 10^5$. As discussed in § 2, these parameters are strongly constrained by the data and have a very small range in which they can vary. We also plot the IC due to the CMB (*dot-dashed line*), the CIB and COB (*red and blue dashed lines*), as well as the maximum expected level of the IC emission due to the optical photons of the host galaxy (*dotted blue line*). The black dotted line marks the 2 yr, 5 σ *Fermi* sensitivity limit. The lower (upper) panel corresponds to the low (high) level EBL.

black solid line is the total SED. The dotted blue line is the IC emission due to the host galaxy optical photons. The IC emission due to the host galaxy IR photons is too weak to appear in the plots. To identify the contribution of the COB and CIB seed photons, we plot with dashed blue and red lines the IC emission due to seed photons with $\lambda < 10$ μm (five short-λ EBL bins in Fig. 2) and with $\lambda > 10$ μm (five long-λ EBL bins in Fig. 2), respectively. We also plot the 2 yr *Fermi* 5 σ sensitivity limit (*dotted black line*). We see that the IC of the EBL plus galaxy seed photons is detectable in both cases, although in the lower EBL case it is only somewhat above the 5 σ limit.

We note that, while the IC emission due to $\lambda > 10$ μm seed photons is CIB-dominated, the COB and galaxy IC contributions from the $\lambda < 10$ μm seed photons are comparable for both low- and high-EBL cases. The IC emission from these seed photons dominates the flux at $\nu \gtrsim 10^{24}$ Hz (corresponding to ~5 GeV), with no contribution from lower energy seed photons. Given that the $\lambda < 10$ μm seed photons are an unspecified mixture of photons from the COB and the host galaxy, a measurement of the IC emission at $\gtrsim$5 GeV energies will provide us only with an upper limit for the COB level. The total emission at energies ~1 to a few GeV is due to comparable contributions of $\lambda < 10$ μm and $\lambda > 10$ μm seed photons. The key in disentangling the contribution of seed photons of different energies is to consider that as the seed photon energy increases, their IC radiation reaches higher energies: at a *Fermi* energy ϵ_γ, only seed photons with energy $\gtrsim \epsilon_\gamma/\gamma^2_{max}$ contribute. This can be used to reconstruct the seed photon SED starting from the optical, needed to model the high-energy part of

TABLE 1

PHOTON INTENSITY IN THE LOBES (IN UNITS OF nW m^{-2} sr^{-1})

Intensity	COB	CIB 1	CIB 2	CIB 3	CIB 4	CIB Total
Initial	142.7	11.0	11.0	27.6	23.0	72.6
Recovered	<159.9	6.4	17.5	26.7	23.0	73.6

Fermi observations, and gradually incorporating lower energy IR seed photons at appropriately chosen levels, to model the emission at gradually lower *Fermi* energies.

We demonstrate now how to recover the EBL from its γ-ray imprint, by breaking the seed photon SED into components of different energy. We anticipate that *Fermi* will detect a steep low-energy tail due to IC-scattered CMB photons, followed by a high-energy hard component due to IC-scattered EBL photons. Let us assume that the EBL is at its maximum level (the procedure we describe also applies to lower EBL levels). This will produce an IC emission at the level shown in the upper panel of Figure 3, and *Fermi* modeling will produce a broken power law (Fig. 4, *dashed line*), soft at low and hard at high energies. As we discussed in § 3, the ~few GeV emission is due to an unspecified mixture of host galaxy optical seed photons and the COB, and modeling it can only provide us with an upper limit for the COB total intensity. We assume for simplicity that the sum of these has a blackbody shape peaking at $\lambda = 1$ μm, and we adjust its amplitude to match the ~5–10 GeV (~10^{24}–$10^{24.5}$ Hz) *Fermi* level. This blackbody intensity is plotted as a solid line at Figure 4*f* and has a total intensity of 159.9 nW m^{-2} sr^{-1}. The resulting IC GeV emission is plotted in Figure 4*a*. Note that our initial COB seed photon intensity in Figure 2 (by summing up the five $\lambda < 10$ μm bins) is 142.7 nW m^{-2} sr^{-1}, below our derived upper limit.

Note that the optical blackbody underproduces the lower energy *Fermi* flux. This cannot be remedied by increasing its normalization, because it would overproduce the ~5–10 GeV flux. Lower energy seed photons are needed. In Figure 4*b*, we include at a low level seed photons at the four bins with $\lambda > 10$ μm. The four thin color lines correspond to the contributions of the same color CIB bins in Figure 4*f*. The dashed red line is the total emission of these four bins, the dashed blue line is the contribution of the 1 μm blackbody, and the black line is the total that has to match the observations. The intensity of the highest frequency seed photon bin (*green*) is adjusted so that the total emission at $\gtrsim 10^{24}$ Hz, the peak energy of this component, matches the observed flux (this produces the small difference between the dashed blue and the black line at $\gtrsim 10^{24}$ Hz). We continue this process in Figures 4*c*–4*e* by increasing the intensity of the other three energy bins, going from higher to lower seed photon energies. The final SED of Figure 4*e* is produced by the photon intensity shown in Figure 4*f*. This is the CIB photon intensity we recovered, and it should be compared to the initial CIB (long-dashed line in Fig. 2) that provided us with the hypothetical *Fermi* observations. The initial seed photon intensities of the COB and CIB, as well as those derived through the above procedure, are given in Table 1. The recovered CIB intensity is close to the initial one, although individual bins can have substantial differences.

This toy-fitting procedure is presented to demonstrate that the CIB (and a COB upper limit) can be recovered from *Fermi* observations and to outline the principles that the actual fitting procedure should incorporate. A more realistic scheme would start with two EBL components (an optical and an IR) and adjust its amplitudes by fitting the *Fermi* SED. One then would split the CIB bin to a subsequently higher number of bins, as long as increasing the number of CIB bins improves substantially the

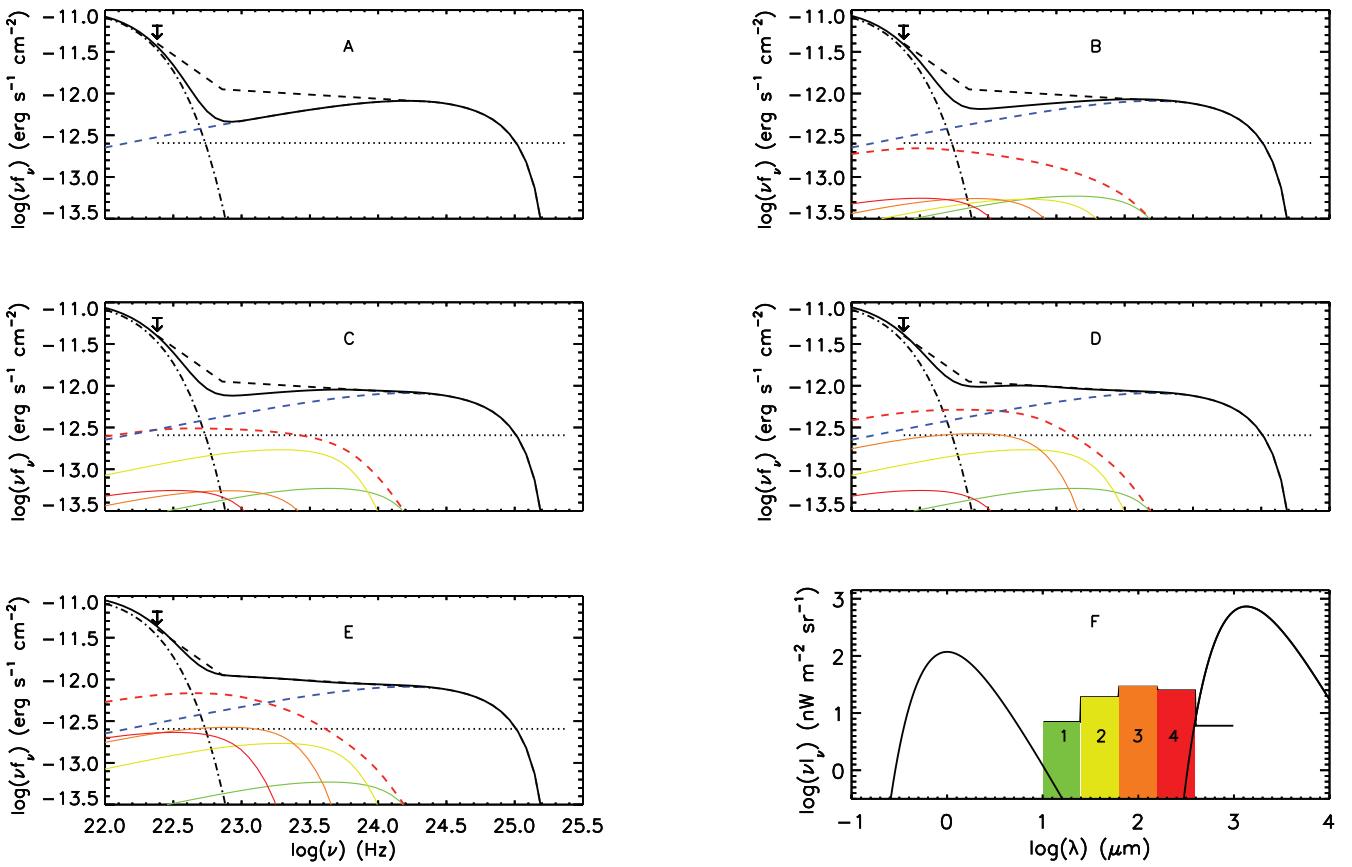

FIG. 4.—How to go from an observed *Fermi* SED to the CIB (see § 3).

fit of the *Fermi* data. In this way, the detail to which we recover the CIB depends on the quality of the *Fermi* data.

4. CONCLUSIONS

We have presented a novel method for measuring the EBL through the detection of the IC emission resulting from the upscattering of EBL photons by relativistic electrons in the lobes of radio galaxies. The requirements that the sources must fulfill (extended, high Galactic latitude, X-ray detection of the IC emission due to CMB seed photons, sharp break of the EED, no significant AGN GeV emission) quickly narrow down the number of candidate sources. Using existing multiwavelength data (radio, *WMAP*, X-ray, EGRET), we show that in the case of Fornax A the EBL imprint is detectable by *Fermi*, even for the lowest expected EBL level. Our method is parameter-free, in the sense that all physical parameters are directly derived from observations. The radiating electron production mechanism (e.g., electron shock acceleration and/or electrons created in hadronic processes) is not relevant for our work, since we derive the EED, regardless of its origin, from multiwavelength data. *Fermi* is observing in scanning mode, so observations of Fornax A are guaranteed. Additional multiwavelength observations in the future can help refine further the derived EBL. We also outline a procedure for solving the inverse problem of going from the upcoming *Fermi* observations to the EBL determination. Our method will determine the CIB (and set upper limits on the COB), finally measuring this cosmologically important quantity.

We thank Nils Odegard for providing the *WMAP* images.

REFERENCES

Aharonian, F., Khangulyan, D., & Costamante, L. 2008, MNRAS, 387, 1206
Aharonian, F., et al. 2006, Nature, 440, 1018
Cheung, C. C. 2007, in ASP Conf. Ser. 373, The Central Engine of Active Galactic Nuclei, ed. L. C. Ho & J.-M. Wang (San Francisco: ASP), 255
Brunetti, G., Setti, G., & Comastri, A. 1997, A&A, 325, 898
Cillis, A. N., Hartman, R. C., & Bertsch, D. L. 2004, ApJ, 601, 142
Dale, D. A., et al. 2007, ApJ, 655, 863
Dermer, C. D., Schlickeiser, R., & Mastichiadis, A. 1992, A&A, 256, L27
Dole, H., et al. 2006, A&A, 451, 417
Erlund, M. C., Fabian, A. C., & Blundell, K. M. 2008, MNRAS, 386, 1774
Feigelson, E. D., Laurent-Muehleisen, S. A., Kollgaard, R. I., & Fomalont, E. B. 1995, ApJ, 449, L149
Finlay, E. A., & Jones, B. B. 1973, Australian J. Phys., 26, 389
Fomalont, E. B., Ebneter, K. A., Van Breugel, W. J. M., & Ekers, R. D. 1989, ApJ, 346, L17
Hauser, M., & Dwek, E. 2001, ARA&A, 39, 249
Hinshaw, G., et al. 2007, ApJS, 170, 288
Isobe, N., Makishima, K., Tashiro, M., Itoh, K., Iyomoto, N., Takahashi, I., & Kaneda, H. 2006, ApJ, 645, 256
Kashlinsky, A. 2005, Phys. Rep., 409, 361
Katarzyński, K., Ghisellini, G., Tavecchio, F., Gracia, J., & Maraschi, L. 2006, MNRAS, 368, L52
Mazin, D., & Raue, M. 2007, A&A, 471, 439
Mills, B. Y., Slee, O. B., & Hill, E. R. 1960, Australian J. Phys., 13, 676
Stecker, F. W., Baring, M. G., & Summerlin, E. 2007, ApJ, 667, L29
Stecker, F. W., de Jager, O. C., & Salamon, M. H. 1992, ApJ, 390, L49